

Self-propagating high-temperature synthesis and solid-phase reactions in bilayer thin films

V. G. Myagkov, V. S. Zhigalov, L. E. Bykova, and V. K. Mal'tsev

*L. V. Kirenskiĭ Institute of Physics, Siberian Branch of the Russian Academy of Sciences,
660036 Krasnoyarsk, Russia*

(Submitted May 13, 1997)

Zh. Tekh. Fiz. **68**, 58–62 (October 1998)

Self-propagating high-temperature synthesis (SHS) in Al/Ni, Al/Fe, and Al/Co bilayer thin films is investigated. It is established that SHS is achieved in thin films at initiation temperatures 300–350° lower than in powders. The mechanism of SHS in thin films is similar to the process of explosive crystallization. It is shown that at the initial stage solid-phase reactions arising on the contact surface of condensate films can be self-propagating high-temperature synthesis. SHS could find application in different technologies for obtaining film components for microelectronics. © 1998 American Institute of Physics. [S1063-7842(98)01010-1]

Self-propagating high-temperature synthesis (SHS) is widely used to obtain many different compounds. Ordinarily, the reagents participating in SHS are in a powdered form or one reagent is in a gaseous state.^{1,2} Infrequently, SHS has been studied in bimetallic systems³ and foils.⁴ In both cases, the reagents were several microns in size. SHS in thin-film samples (thickness up to 200 nm) has not been investigated at all.

The present work is devoted to the experimental study of the characteristic features of SHS in thin films and their differences from SHS in powders.

The following pairs were chosen as the initial materials for synthesis: Ni–Al, Fe–Al, and Co–Al. A layer of one of the ferromagnetic metals $M = \text{Ni, Fe, and Co}$ was deposited successively by thermal evaporation and an Al layer was deposited on top. Each layer was 30–100 nm thick. Films with layers of equal thickness were used for the investigations; this corresponds to ~40% at Al in the sample. Mica or glass, 0.1–0.2 mm thick with linear dimensions of 5–10 mm, was used as the substrate. The two-layer system obtained was placed on a tungsten heater and heated at a rate of the order of 20° per second (thermal explosion). The vacuum during deposition and heating was 1×10^{-4} Pa. At the temperature T_{li} a nucleus of a phase of the reaction products appeared and propagated with the velocity $V \sim 0.5 \times 10^{-2}$ m/s until it covered the entire surface of the film. The morphology of the surface of the new phase changed, and the reflection from the film surface became dull and differed sharply from the mirror surface of the initial sample, so that the motion of the new phase was easily observed visually (Fig. 1a). The initiation temperature T_{li} in the experiments was not constant; it depended on the rate of heating and the ratio of the thicknesses of each film and varied in the range 250–400 °C for the systems Co–Al and Fe–Al and 200–300 °C for Ni–Al. If t is the characteristic reaction time, then the velocity of the front is $V \sim \sqrt{\chi/t}$. In this time the diffusion will extend to the thickness of the film $d \sim \sqrt{Dt}$. Taking average experimental values $V = 1 \times 10^{-2}$ m/s, $d = 1 \times 10^{-7}$ m, and thermal diffusivity $\chi = 10^{-5} - 10^{-6}$ m²/s

(Ref. 5), we estimate the diffusion coefficient as $D = 10^{-12} - 10^{-13}$ m²/s. Such values of D are characteristic for the Al diffusion in Fe, Co, or Ni at temperature 1200–1400 K.⁶ This temperature agrees with the results of direct measurements, presented below, of the temperature of an Al/Fe film. Hence it follows that at these temperatures Al on the front is in a liquid state, while the lower Fe, Co, or Ni layers are in a solid phase. The reaction front is convex (Fig. 1a), because of the fact that the heat losses at the edge of the film are greater than at the center. They decrease the front temperature T_f and the front velocity from center to edge. On the other hand, the front temperature is higher than the melting temperature of aluminum T_m (Al). The arrow in Fig. 1a shows the liquid zone of aluminum, bordering the reaction front and possessing a high reflectance, so that it is distinguished from the initial and reacted parts of the film. If, after initiation, the substrate temperature is made to be less than T_{li} , then quenching of the reaction occurs.

The self-maintaining character of the propagation of the nucleus is determined by the fact that the reaction zone lies at the interface of the initial film and the reaction products. Intense heat release on the front appreciably raises the temperature there. As a result of the Arrhenius temperature dependence of the diffusion coefficient the combustion process proceeds exclusively on the front. The proposed mechanism of SHS in thin films is similar to the process of autowave oxidation of metals^{7,8} and the process of explosive crystallization.^{9,10} The main characteristics of the processes are similar in the following cases: the existence of the reaction initiation temperature T_{li} , self-maintained propagation of the front of a new phase, high temperature of the front, identical temperature dependences of the front propagation velocity, and possibility of the existence of a liquid zone on the front. The process of explosive crystallization has been well studied theoretically, so that it can be applied to the analysis of phenomena arising during SHS in thin films and autowave oxidation of metals. Figure 1b shows schematically the temperature profile on the reaction front, which, assuming that no phase transformations occur, is

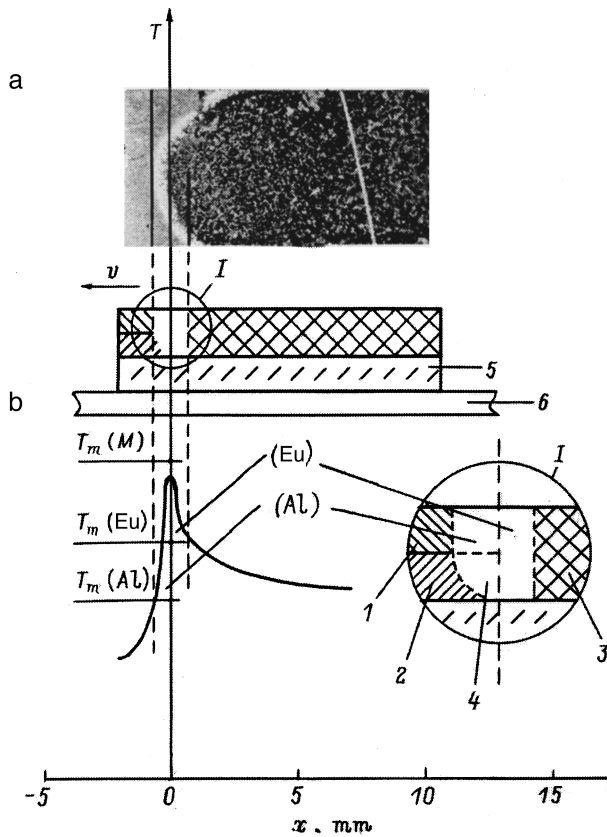


FIG. 1. Photograph, schematic illustration of SHS with a liquid aluminum zone, which is shown by the arrow, on the front (a), and temperature profile, perpendicular to the reaction front, with a liquid aluminum zone at the front (b): 1 — Al film; 2 — metal film $M = \text{Fe, Co, Ni}$; 3 — reaction products; 4 — liquid zone on the SHS front; 5 — substrate; 6 — heater at temperatures $T > T_{2i}$.

exponential.¹¹ The front temperature T_f lies in the range $T_m(M) > T_f > T(\text{Al})$, so that a liquid phase of aluminum exists at the front. Aluminum diffuses into the bottom metal layer ($M = \text{Ni, Fe, Co}$), which is in the solid phase. If the lowest eutectic temperature $T_m(\text{Eu})$ of the reaction products is less than the front temperature $T_f > T_m(\text{Eu})$, then the liquid zone should include, besides liquid aluminum (Al), liquid reaction products (Eu). The width of the liquid zone depends on the temperature profile of the reaction front (Fig. 1b).

The magnetic moment $M(T_i)$ of the sample was measured in the experiments. It is proportional to the volume of the ferromagnetic part of the film, depending on the substrate temperature. The degree of transformation $\eta(T_i) = (M(0) - M(T_i))/M(0)$ was determined assuming all intermetallic phases of Al with Ni, Co, and Fe to be nonmagnetic. Here $M(0)$ is the magnetic moment of the initial sample at room temperature and $M(T_i)$ is the magnetic moment after the substrate is heated to temperature T_i and held for 10 s — the time required for the combustion wave to propagate through the film. Figure 2 shows the dependence $\eta(T_i)$ for the systems Ni–Al, Co–Al, and Fe–Al. From the dependence $M(T_i)$ follows the existence of the synthesis onset temperature T_{1i} and temperature T_{2i} at which the degree of transformation has a maximum value. In Fig. 2 the temperatures T_{1i} and T_{2i} are marked only for Al/Ni films. Thus, at tempera-

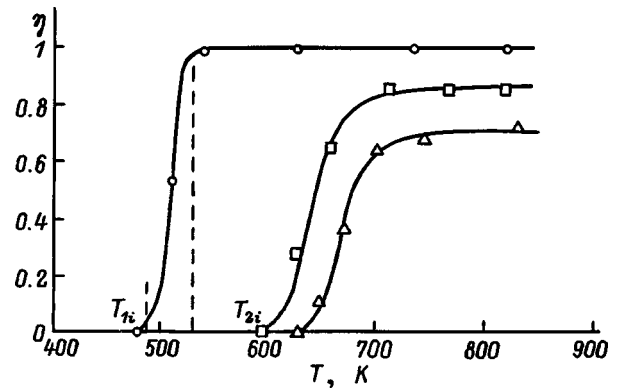


FIG. 2. Degree of transformation of bilayer systems as a function of substrate temperature: \circ — Al/Ni, \square — Al/Fe, \triangle — Al/Co; layer thicknesses: Al ~ 60 nm, $M \sim 50$ nm.

tures $T > T_{2i}$ nickel reacts completely with aluminum, and there is not enough time for 0–30% of the cobalt and 0–20% of the iron to react. Analysis of the surface morphology suggests that in the temperature range $T_{2i} > T > T_{1i}$ synthesis does not proceed to the entire depth, but covers a thickness d at the interface of the films. The thickness d increases rapidly with increasing substrate temperature, and at temperature T_{2i} synthesis proceeds to the entire depth. The large fraction of the surface where the reagents are in contact with one another decreases appreciably the initiation temperature T_{1i} . For the system Ni–Al this temperature is 300–350° lower than the corresponding temperature in powders.^{11,12} In many technologies for obtaining thin-film coatings, the films cool down at substrate temperatures higher than the initiation temperature T_{1i} . This suggests that if the substrate temperature T_i is higher than the initiation temperature T_{1i} when the multilayer films are deposited, SHS can proceed and change the expected phase composition and structure of the samples. To confirm this conjecture, an Al layer (~ 50 nm thick) at different substrate temperatures was deposited on Co, Ni, Fe films (~ 50 nm thick) deposited on mica substrates. The degree η of transformation was determined as a function of the substrate temperature T_i by the method presented above. Figure 3 shows the dependence $\eta(T_i)$, which shows that the SHS process is initiated during deposition of the upper layer

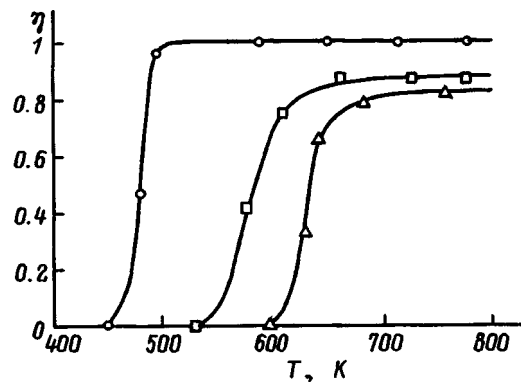


FIG. 3. Degree of transformation versus substrate temperature after deposition of an Al layer on a film $M = \text{Ni, Fe, Co}$: \circ — Al/Ni, \square — Al/Fe, \triangle — Al/Co.

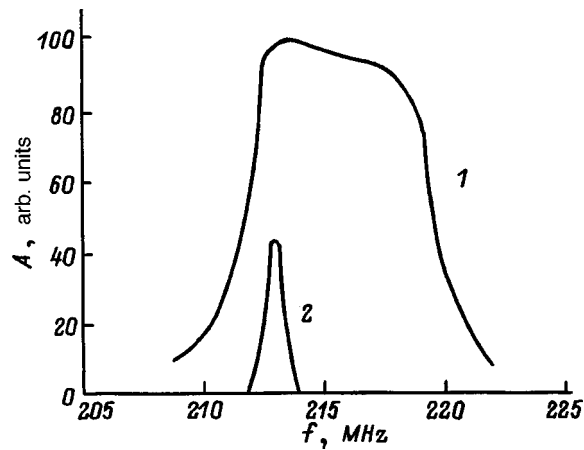


FIG. 4. Frequency spectra of nuclear spin echo of a bilayer film system Al/Co: 1 — initial sample, 2 — after passage of a SHS wave through the sample.

of aluminum. In addition, the initiation temperatures of the systems Ni–Al, Fe–Al, and Co–Al are close to the corresponding temperatures during heating of bilayer films of the same systems (Fig. 2).

Al/Co bilayer film systems were also investigated by the nuclear magnetic resonance method. Figure 4 shows the frequency spectra of the nuclear spin echo (NSE) of the initial films and of the same samples after annealing, where SHS was realized. The typical Al/Co spectrum of the initial samples is characteristic for polycrystalline Co and is formed by two of its allotropic modifications: the low-temperature hexagonal close-packed (hcp) α -Co phase and the high-temperature face-centered cubic (fcc) β -Co phase (the $\alpha \rightleftharpoons \beta$ transition temperature ~ 700 K) with central frequency 213 MHz. After passage of the SHS wave the line shape of the spectrum changes appreciably, and only the signal from the fcc phase remains. The reaction products experience high rates of cooling, which results in, specifically, stabilization of the high-temperature fcc phase of Co. Thus, taking the rise in temperature in the combustion wave $\Delta T \sim 1000$ K and the characteristic reaction time $t = \chi/v^2 \sim 0.1 - 0.01$ s we estimate the cooling rate as $\sim 10^4 - 10^5$ K/s. Such cooling rates are sufficient not only for fixing the high-temperature phases but also for obtaining an amorphous phase in the alloys. The absence of satellite lines in the low-frequency region of the spectrum shows that after the passage of a SHS wave a solid solution of aluminum in cobalt is not formed, but rather intermetallic compounds are formed. The area under the curve of the frequency spectrum determines the amount of cobalt present in the sample. The degrees of transformation, determined from the ratio of the areas of the spectra before and after the reaction and from magnetic measurements, agree well with one another.

The phase composition of the samples after the passage of a SHS wave was investigated by the methods of x-ray crystallographic analysis. The samples investigated had layers of equal thicknesses, each layer being ~ 100 nm thick. The diffraction patterns of the samples of the system Al/Ni where SHS occurred as a result of annealing at temperature $T > T_{2i}$ are completely identical to the diffraction patterns of

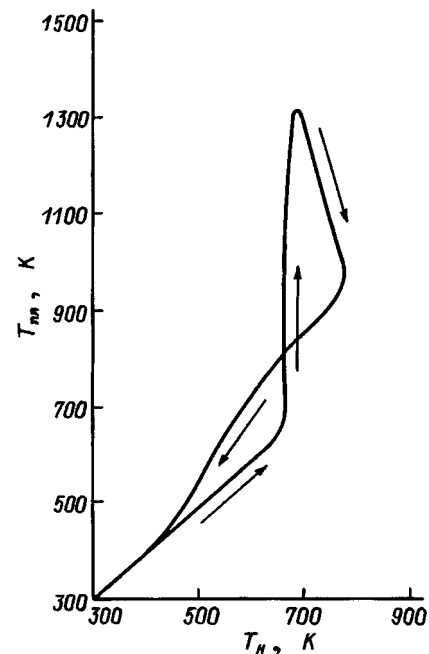


FIG. 5. Temperature of a bilayer film sample Al/Fe versus the heater temperature. The arrows show the path of the temperature as the sample is heated up to 770 K and then cooled.

samples where SHS occurred with an aluminum film deposited on a nickel film at temperature $T > T_{2i}$. The interpretation of the diffraction patterns shows the presence of a main phase Ni_2Al_3 with a small quantity of a NiAl phase and show residual aluminum and nickel to be absent, in agreement with the data presented in Figs. 2 and 3. For Al/Fe films where SHS occurred as a result of annealing the diffraction patterns show reflections from residual α -Fe as well as the high-temperature phase γ -Fe and the intermetallic compounds FeAl_3 and Fe_2Al_5 . The high-temperature phase γ -Fe was stabilized just as β -Co as a result of the high rates of cooling which arise on the combustion front. Similar diffraction patterns of Al/Co samples, just as their magnetic measurements and NMR spectra, confirmed the presence of residual β -Co. In addition, other phases, which can be identified as Al_5Co_2 and AlCo, are present in the sample.

The film temperature during passage of a SHS wave was measured in the system Al/Fe. To this end, a Pd layer (50 nm thick) was deposited on the substrate and Fe and Al layers (each layer 50 nm thick) were deposited successively on the Pd layer. The Pd and Fe layers were used as thermocouples. The sample was placed on a heater whose temperature was determined with a standard chromel–copel thermocouple and heated at rate 10 K/s. The heater was switched off at temperature 770 K, which is higher than the initiation temperature T_{1i} . Figure 5 shows the dependence of the sample temperature measured with the film thermocouple on the heater temperature. Before the temperature T_{1i} was reached, both thermocouples showed the same temperature. This signified that the heater temperature was identical to the film temperature. However, above $T_{1i} = 660$ K the film temperature increased rapidly to a value of the order of 1330 K as a result of an exothermic reaction. This value agrees well

with the estimate of the front temperature made earlier. After the passage of the SHS wave, the temperature indicated by the film thermocouple dropped. However, the reverse path of the film temperature was different from the forward path and was higher than the heater temperature, which indicated continuation of the exothermic reaction. The reaction stops only at temperatures 300–350 K, and the film and heater temperatures become the same.

To determine the total reaction time the electrical resistance of the samples during the reaction at temperature T_{1i} was measured. The electrical resistance increases continuously as the temperature increases from room temperature to T_{1i} . This increase is typical for the temperature dependence of the resistance of metals. When the temperature reaches the initiation value T_{1i} the electrical resistance of the sample increases rapidly — for 20 min for Al/Co systems and for 10 min for Al/Ni, Al/Fe film systems. Experiments to determine the sample temperatures and electrical resistance show that after the passage of a SHS wave through the film (for the present samples not more 10 s), the further heat release in the film is due to a post-combustion process. Post-combustion processes have been observed in previous works on SHS.² Hence it follows that the reaction process consists of two stages. During the first stage a fast autowave combustion process occurs. It results in appreciable mixing of the reagent layers and formation of reaction products. The second stage is slower. At this stage the initial products that have not completely reacted in the first stage undergo post-combustion. This stage can be accompanied by recrystallization and formation of new phases. During the second stage the combustion process is not a wave process, but rather the reaction products are produced by a process of nucleation and growth, whose kinetic law is described by the Kolmogorov–Avrami–Johnson–Mehl equation.¹³

The low initiation temperatures of SHS in bilayer film systems suggest that many solid-phase reactions in the initial stage at the interface of film condensates are self-propagating high-temperature synthesis. Thus, in Ref. 14 solid-phase reactions were investigated in Ni/Al multilayer films. Similarly to the present work, solid-phase Ni/Al reactions in multilayers materialize both as a result of annealing and during combined deposition of nickel and aluminum films. The fact that in our work and in Ref. 14 the initiation temperatures of the reactions $T_{1i} \sim 500$ K are the same suggests that SHS in multilayer films was also observed in the work mentioned. For this reason, it should be expected that other solid-phase reactions arising at the contact surface of film condensates can initially be self-propagating high-temperature synthesis. This is the reason for the search for solid-phase reactions that

could be realized in bilayer film samples. They should occur in systems where SHS has been obtained.¹ Conversely, for films on whose boundary solid-phase reactions arise (see, for example, Ref. 15) SHS should be expected to occur in the corresponding powders.

The following conclusions can be drawn on the basis of the initial experiments investigating SHS in thin films: 1) SHS materializes in thin films at initiation temperatures 300–350° lower than in powders; 2) the mechanism of SHS in thin films is similar to explosive crystallization; 3) SHS in thin films can also be obtained on the surface of powders if a second reagent in a liquid phase is present; 4) the possibility of SHS initiation should be taken into account in existing technologies for obtaining thin-film coatings; 5) different solid-phase reactions observed at the interface of bilayer and multilayer films and arising at low heat-treatment temperatures can initially be self-propagating high-temperature synthesis; 6) the high rates of cooling after the passage of a SHS wave in bilayer film samples can stabilize high-temperature and metastable phases; and, 7) SHS could find application in different technologies for obtaining film components for microelectronics.

This work was supported by the Russian Fund for Fundamental Research, Grant No. 96-32327a/410.

¹A. G. Merzhanov, in *Physical Chemistry* [in Russian], edited by Kolotykin, Khimiya, Moscow (1983), pp. 6–45.

²A. G. Merzhanov and I. P. Borovinskaya, *Dokl. Akad. Nauk SSSR* **204**, 366 (1972) [*Dokl. Chem.* **201**, 429 (1972)].

³S. G. Vadchenko, A. M. Bulaev, Yu. A. Gal'chenko, and A. G. Merzhanov, *Fiz. Goren. i Vzryva*, No. 6, 46 (1987).

⁴U. Anselmi-Tamburini and Z. A. Munir, *J. Appl. Phys.* **66**, 5039 (1989).

⁵I. S. Grigor'ev and E. Z. Meilikhov [Eds.], *Physical Constants* [in Russian], Energoatomizdat, Moscow (1991), 1232 pp.

⁶V. N. Larikov and V. I. Isaichev, *Structure and Properties of Metals and Alloys. Diffusion in Metals and Alloys* [in Russian], Naukova Dumka, Kiev (1987), 511 pp.

⁷V. G. Myagkov, L. I. Kveglis, G. I. Frolov, and V. S. Zhigalov, *J. Mater. Sci. Lett.* **13**, 1284 (1994).

⁸V. G. Myagkov and N. V. Baksheev, *Pis'ma Zh. Tekh. Fiz.* **18**(6), 14 (1992) [*Sov. Tech. Phys. Lett.* **18**(3), 174 (1992)].

⁹V. A. Shklovskii and V. M. Kuz'menko, *Usp. Fiz. Nauk* **157**, 311 (1989) [*Sov. Phys. Usp.* **32**, 163 (1989)].

¹⁰G. H. Gilmer and H. J. Leamy, in *Laser and Electron-Beam Processing of Materials*, Academic Press, New York (1980), pp. 227–232.

¹¹K. A. Philpoh, Z. A. Munir, and J. B. Holt, *J. Mater. Sci.* **22**, 159 (1987).

¹²C. Michaelson, G. Lucadamo, and K. Barmak, *J. Appl. Phys.* **80**, 6689 (1996).

¹³R. W. Cahn and P. Haasen [Eds.], *Physical Metallurgy*, (North-Holland, New York, 1983, Vol. 2; Mir, Moscow, 1968), 490 pp.

¹⁴E. O. Coldan, C. Cabral, Kotecki Jr. *et al.*, *J. Appl. Phys.* **77**, 614 (1995).

¹⁵L. Persson, M. El. Bouanani, and M. Hult *et al.*, *J. Appl. Phys.* **80**, 3347 (1996).